The current issue and full text archive of this journal is available at
www.emeraldinsight.com/0961-5539.htm

Heat and mass transfer from truncated cones with variable wall temperature and concentration in the presence of chemical reaction effects

Received 8 May 2010
Revised 23 August 2010
Accepted 20 October 2010

Ali J. Chamkha
Manufacturing Engineering Department, The Public Authority for Applied Education and Training, Shuweikh, Kuwait

A.M. Rashad
Department of Mathematics, South Valley University, Aswan, Egypt, and

Humood F. Al-Mudhaf
Chemical Engineering Department, The Public Authority for Applied Education and Training, Shuweikh, Kuwait

Abstract

Purpose – The purpose of this paper is to solve the problem of steady, laminar, coupled heat and mass transfer by MHD natural convective boundary-layer flow over a permeable truncated cone with variable surface temperature and concentration in the presence of thermal radiation and chemical reaction effects.

Design/methodology/approach – The governing equations are derived and transformed into a set of non-similar equations which are then solved by an adequate implicit finite difference method.

Findings – It is found that the presence of thermal radiation, magnetic field and chemical reaction have significant effects on the rates of heat and mass transfer. The variation of the wall temperature and concentration exponent contribute to significant changes in the Nusselt and Sherwood numbers as well.

Originality/value – The titled problem with the various considered effects has not been solved before and it is of special importance in various industries. The problem is original.

Keywords Heat transfer, Mass transfer, Chemical reactions, Boundary layers, Flow

Paper type Research paper

Nomenclature

a_r = Rosseland mean extinction coefficient
B_o = magnetic induction
c_p = specific heat at constant pressure
C_f = local skin-friction coefficient, $2\nu(\partial u/\partial y)_{y=0}/U_r^2$
D = mass diffusivity
f = dimensionless stream function
f_o = wall mass transfer coefficient, $v_o/\nu(x_o^4/Gr_{x_o})^{1/4}$
g = gravitational acceleration
Gr_{x*} = local Grashof number, $g\cos\gamma\beta_T(T_w - T_\infty)(x^*)^3/\nu^2$
h = local heat transfer coefficient
h_m = local mass transfer coefficient
k = thermal conductivity
k_r = dimension of chemical reaction
Ha = Hartmann number, $(\sigma^* B_o^2/(\rho v)(x_o^4/Gr_{x_o})^{1/2})^{1/2}$

International Journal of Numerical Methods for Heat & Fluid Flow
Vol. 22 No. 3, 2012
pp. 357-376

0961-5539
DOI 10.1108/09615531211208060

N = concentration to thermal buoyancy ratio, $\beta_c(c_w - c_\infty)/(\beta_T(T_w - T_\infty))$
Nu_{x^*} = local Nusselt number, hx^*/k
Pr = Prandtl number, ν/α
r = local radius of the truncated cone
r_t = surface temperature parameter, T_w/T_∞
R_d = radiation-conduction parameter, $4\sigma T_\infty^3/[k(a_r + \sigma_s)]$
Sc = Schmidt number, ν/D
Sh_{x^*} = local Sherwood number, $h_m x^*/D$
T = temperature
u = velocity component in the x-direction
U_r = reference velocity, $[g\cos\gamma\beta_T (T_w - T_\infty)x^*]^{1/2}$
v = velocity component in the y-direction
v_o = wall suction or injection velocity
x = streamwise coordinate
x_o = distance of the leading edge of truncated cone measured from the origin
x^* = distance measured from the leading edge of the truncated cone, $x - x_o$
y = transverse coordinate

Greek symbols
α = thermal diffusivity
β_c = coefficient of concentration expansion
β_T = coefficient of thermal expansion
γ = dimensionless of chemical reaction
η = pseudo-similarity variable
ϕ = dimensionless concentration, $(c - c_\infty)/(c_w - c_\infty)$
θ = dimensionless temperature, $(T - T_\infty)/(T_w - T_\infty)$
ξ = dimensionless distance
ν = kinematic viscosity
Ω = half angle of the truncated cone
ρ = density
σ = Stefan-Boltzmann constant
σ^* = electrical conductivity
σ_s = scattering coefficient
ψ = stream function

Subscripts
w = condition at the wall
∞ = condition at infinity

Introduction

Natural convection induced by the simultaneous action of buoyancy forces resulting from thermal and mass diffusion is of considerable interest in nature and in many industrial applications such as meteorology, chemical industry, solar physics, cooling of nuclear reactors, cosmic fluid dynamic, astrophysics, geophysics, magnetohydrodynamic (MHD) power generators and in the earth's core. Many studies that considered combined heat and mass transfer in natural convection boundary-layer flows over heated surfaces with various geometries can be found in the monograph by Gebhart *et al.* (1998). Also, many researches have been carried out to include various physical aspects of the problem of combined heat and mass transfer about cones. For example, Na and Chiou (1979) studied laminar natural convection over a frustum of a cone. Pop and Na (1999) presented a numerical solution of the problem of natural convection over a vertical wavy frustum of a cone. Yih (1999) examined the effect of radiation on natural convection about a truncated cone. Chamkha (2001) examined coupled heat and mass transfer by natural convection about a truncated cone in the presence of magnetic field and radiation effects. Postelnicu (2006) studied free convection about a vertical frustum of a cone in a micropolar fluid. Recently, Cheng (2008) analyzed natural convection heat transfer near a vertical truncated cone with power-law variation in surface temperature in a micropolar fluid. Cheng (2009) also studied natural convection heat and mass transfer from a vertical truncated cone in a porous medium saturated with a non-Newtonian fluid with variable wall temperature and concentration.

Moreover, combined heat and mass transfer problems with chemical reaction are of importance in many processes and have, therefore, received a considerable amount of attention in recent years. In processes such as drying, evaporation at the surface of a water body, energy transfer in a wet-cooling tower, and the flow in a desert cooler,

heat and mass transfer occur simultaneously. Possible applications of this type of flow can be found in many industries. For example, in the power industry, among the methods of generating electric power is one in which electrical energy is extracted directly from a moving conducting fluid. Many practical diffusive operations involve the molecular diffusion of a species in the presence of chemical reaction within or at the boundary. There are two types of chemical reactions. A homogeneous chemical reaction is one that occurs uniformly throughout a given phase. The species generation in a homogeneous chemical reaction is analogous to internal source of heat generation. In contrast, a heterogeneous chemical reaction takes place in a restricted region or within the boundary of a phase. It can, therefore, be treated as a boundary condition similar to the heat flux condition in heat transfer. The study of heat and mass transfer with chemical reaction is of great practical importance to engineers and scientists because of its almost universal occurrence in many branches of science and engineering. Soundalgekar (1977) presented an exact solution to the flow of a viscous fluid past an impulsively started infinite with constant heat flux and chemical reaction. The solution was derived by the Laplace transform technique and the effects of heating or cooling of the plate on the flow field were discussed through the Grashof number. Das *et al.* (1994) studied the effects of mass transfer on the flow past an impulsively started infinite vertical plate with constant heat flux and chemical reaction. Muthucumaraswamy and Ganesan (1998) considered the problem of unsteady flow past an impulsively started isothermal vertical plate with mass transfer by an implicit finite-difference method. Muthucumarswamy and Ganesan (2001, 2002) solved the problem of unsteady flow past an impulsively started vertical plate with uniform heat and mass flux and variable temperature and mass flux, respectively. Diffusion of a chemically reactive species from a stretching sheet was studied by Andersson *et al.* (1994). Anjalidevi and Kandasamy (1999, 2000) analyzed the effects of chemical reaction, heat and mass transfer on laminar flow without or with MHD along a semi infinite horizontal plate.

Finally, thermal radiation effects with chemical reactions on free convection flow and mass transfer have importance in such processes as the combustion of fossil fuels, atmospheric re-entry with suborbital velocities, plasma wind tunnels, electric spacecraft propulsion, hypersonic flight through planetary atmosphere photo-dissociation, photo ionization, and geophysics. Analytical solutions for the overall heat and mass transfer on MHD flow of a uniformly stretched vertical permeable surface with the effects of heat generation/absorption and chemical reaction were presented by Chamkha (2003). The effects of radiation and chemical reaction on MHD free convective flow and mass transfer past a vertical isothermal cone surface were investigated by Afify (2004). Kandasamy *et al.* (2005) studied the nonlinear MHD flow with heat and mass transfer characteristics on a vertical stretching surface with chemical reaction and thermal stratification effects. The effects of chemical reaction and the thermal radiation on hydromagnetic mixed convection heat and mass transfer for Hiemenz flow through porous media in the presence of variable viscosity and magnetic field were considered by Seddeek (2005). Ibrahim *et al.* (2008) studied the effect of the chemical reaction and radiation absorption on the unsteady MHD free convection flow past a semi infinite vertical permeable moving plate with heat source and suction. Mohamed and Abo-Dahab (2009) studied the effect of the first-order chemical reaction and thermal radiation on the heat and mass transfer in MHD micropolar fluid flow over a vertical moving porous plate through a porous medium. Pal and Talukdar (2010a) investigated

the combined effects of thermal radiation and first-order chemical reaction on the heat and mass transfer by MHD mixed convection flow past a permeable vertical plate embedded in a porous medium. Pal and Talukdar (2010b) investigated the influence of thermal radiation and magnetic field on the steady combined heat and mass by mixed convection along a semi-infinite vertical plate taking into account a homogeneous chemical reaction of first order. Chamkha and Al-Mudhaf (2004) investigated coupled heat and mass transfer by natural convection from a permeable sphere in the presence of an external magnetic field and thermal radiation effects. The effects of thermal radiation and magnetic field on natural convection heat transfer from a vertical flat plate embedded in a fluid-saturated porous medium were analyzed by Rashad (2008).

Hence, the purpose of the present work is to study the effects of chemical reaction and thermal radiation on the coupled heat and mass transfer by MHD natural convection boundary-layer flow over a permeable truncated cone with variable surface temperature and concentration. The governing boundary-layer equations have been transformed into a non-similar form, and these have been solved numerically. The effects of magnetic field, thermal radiation, chemical reaction, injection or suction and power-law variations of both the wall temperature and concentration on the velocity, temperature and concentration profiles as well as the local skin-friction coefficient, local Nusselt number and the local Sherwood number have been shown graphically and discussed.

Governing equations

Consider steady, laminar, heat and mass transfer by natural convection, boundary layer flow of an electrically conducting and optically dense fluid about a truncated permeable cone with a half angle Ω in the presence of thermal radiation and chemical reaction effects as shown in Figure 1. The origin of the coordinate system is placed at the vertex of the full cone where x represents the distance along the cone and y represents the distance normal to the surface of the cone. The cone surface is maintained at a variable

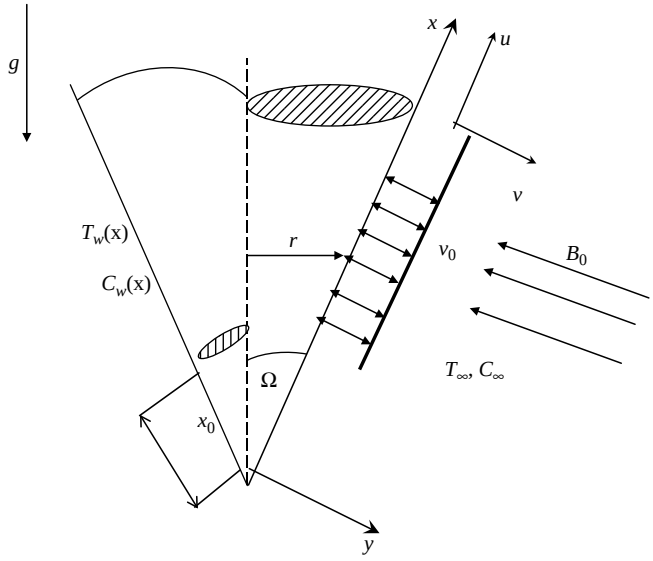

Figure 1.
Problem schematics and coordinate system

temperature $T_w(x)$ and a variable concentration $c_w(x)$ and the ambient temperature and concentration far away from the surface of the cone T_∞ and c_∞ are assumed to be uniform. For $T_w > T_\infty$ and $c_w > c_\infty$ an upward flow is induced as a result of the thermal and concentration buoyancy effects. $T_w(x)$ and $c_w(x)$ are assumed to vary as power-law functions of the distance along the cone surface x. Fluid suction or injection is imposed at the surface. A uniform magnetic field is applied in the *y*-direction normal to the flow direction. The magnetic Reynolds number is assumed to be small so that the induced magnetic field is neglected. In addition, the Hall effect and the electric field are assumed negligible. The small magnetic Reynolds number assumption uncouples the Navier-Stokes equations from Maxwell's equations. A first-order homogeneous chemical reaction is assumed to take place in the flow. All physical properties are assumed constant except the density in the buoyancy force term. By invoking all of the boundary layer, Boussineq and Rosseland diffusion approximations (see, for instance, Yih (1999) and Chamkha (2001) the governing equations for this investigation can be written as:

$$\frac{\partial(\mathrm{ru})}{\partial \mathrm{x}} + \frac{\partial(\mathrm{rv})}{\partial \mathrm{y}} = 0 \tag{1}$$

$$u\frac{\partial u}{\partial x} + v\frac{\partial u}{\partial y} = \nu\frac{\partial^2 u}{\partial y^2} + g\beta_T(T - T_\infty)\cos\Omega + g\beta_c(c - c_\infty)\cos\Omega - \frac{\sigma^* B_o^2}{\rho}u \tag{2}$$

$$\mathrm{u}\frac{\partial \mathrm{T}}{\partial \mathrm{x}} + \mathrm{v}\frac{\partial \mathrm{T}}{\partial \mathrm{y}} = \alpha\frac{\partial^2 \mathrm{T}}{\partial \mathrm{y}^2} + \frac{16\sigma}{3(\mathrm{a_r} + \sigma_\mathrm{s})\rho \mathrm{c_p}}\frac{\partial}{\partial \mathrm{y}}\left(\mathrm{T}^3\frac{\partial \mathrm{T}}{\partial \mathrm{y}}\right) \tag{3}$$

$$\mathrm{u}\frac{\partial \mathrm{c}}{\partial \mathrm{x}} + \mathrm{v}\frac{\partial \mathrm{c}}{\partial \mathrm{y}} = \mathrm{D}\frac{\partial^2 \mathrm{c}}{\partial \mathrm{y}^2} - \mathrm{k_r}(\mathrm{c} - \mathrm{c}_\infty) \tag{4}$$

where r is the radius of the truncated cone. u, v, T, and c are the x-component of velocity, y-component of velocity, temperature, and concentration, respectively. ρ, ν, c_p, α, and D are the fluid density, kinematic viscosity, specific heat at constant pressure, thermal diffusivity and mass diffusivity, respectively. σ^*, B_o, β_T and β_c are the fluid electrical conductivity, magnetic induction, thermal expansion coefficient and concentration expansion coefficient, respectively. g, σ, σ_s, and a_r are the acceleration due to gravity, Stefan-Boltzmann constant, scattering coefficient, and the Rosseland mean extinction coefficient, respectively. k_r is the chemical reaction rate. The coefficient of the last term of equation (3) is some times termed as the radiative conductivity as mentioned by Yih (1999).

The boundary and ambient conditions for this problem can be written as:

$$\begin{aligned} &y = 0 : u = 0, \quad v = -v_o, \quad T = T_w(x) = T_\infty + a_1(x - x_o)^n, \\ &c = c_w(x) = c_\infty + b_1(x - x_o)^n \end{aligned} \tag{5}$$

$$\mathrm{y} \to \infty : \mathrm{u} \to 0, \quad \mathrm{T} \to \mathrm{T}_\infty, \quad \mathrm{c} \to \mathrm{c}_\infty \tag{6}$$

where a_1, b_1 and n are constants and v_o represents the transpiration velocity of fluid through the surface of the cone or the permeability of the porous surface where its sign indicates suction or withdrawal of fluid when $v_o > 0$ and blowing or injection of fluid when $v_o < 0$. The case $v_o = 0$ indicates that the cone surface is impermeable.

The governing equations and boundary conditions can be made dimensionless by introducing the stream function such that:

$$\mathrm{ru} = \frac{\partial \psi}{\partial \mathrm{y}}, \quad \mathrm{rv} = -\frac{\partial \psi}{\partial \mathrm{x}} \tag{7}$$

and using the following dimensionless variables:

$$\xi = \frac{\mathrm{x} - \mathrm{x_o}}{\mathrm{x_o}} = \frac{\mathrm{x}^*}{\mathrm{x_o}}, \quad \eta = \frac{\mathrm{y}}{\mathrm{x}^*}(\mathrm{Gr_{x\bullet}})^{1/4}, \quad \mathrm{Gr_{x\bullet}} = g\beta_T(\mathrm{T_w} - \mathrm{T_\infty})\mathrm{x}^{*3}/\nu^2$$

$$\mathrm{f}(\xi, \eta) = \frac{\psi}{\mathrm{r}\nu(\mathrm{Gr_{x\bullet}})^{1/4}}, \quad \theta(\xi, \eta) = \frac{\mathrm{T} - \mathrm{T_\infty}}{\mathrm{T_w} - \mathrm{T_\infty}}, \quad \phi(\xi, \eta) = \frac{\mathrm{c} - \mathrm{c_\infty}}{\mathrm{c_w} - \mathrm{c_\infty}} \tag{8}$$

$$u = \frac{\nu(Gr_{x\bullet})^{1/2}}{x^*} f' = U_r f', \quad v = -\frac{\nu(Gr_{x\bullet})^{1/4}}{x^*}\left[\left(\frac{\xi}{1+\xi} + \frac{3+n}{4}\right) f + \xi\frac{\partial f}{\partial \xi} - \frac{1}{4}\eta f'\right]$$

where $\mathrm{U_r}$ is a reference velocity.

Substituting equations (7) and (8) into equations (1)-(6) yields the following non-similar dimensionless equations:

$$f''' + \left(\frac{\xi}{1+\xi} + \frac{3+n}{4}\right) ff'' - \frac{1+n}{2}(f')^2 - Ha^2\xi^{1/2}f' + \theta + N\phi = \xi\left(f'\frac{\partial f'}{\partial \xi} - f''\frac{\partial f}{\partial \xi}\right), \tag{9}$$

$$\frac{\theta''}{\mathrm{Pr}} + \left(\frac{\xi}{1+\xi} + \frac{3+n}{4}\right) f\theta' - nf'\theta + \frac{4}{3}\frac{R_d}{\mathrm{Pr}}\left\{\theta'[(r_t - 1)\theta + 1]^3\right\}' = \xi\left(f'\frac{\partial \theta}{\partial \xi} - \theta'\frac{\partial f}{\partial \xi}\right), \tag{10}$$

$$\frac{\phi''}{Sc} + \left(\frac{\xi}{1+\xi} + \frac{3+n}{4}\right) f\phi' - nf'\phi - \gamma\xi^{1/2}\phi = \xi\left(f'\frac{\partial \phi}{\partial \xi} - \phi'\frac{\partial f}{\partial \xi}\right), \tag{11}$$

$$\eta = 0 : f' = 0, \quad f_o\xi^{1/4} = \left(\frac{\xi}{1+\xi} + \frac{3+n}{4}\right) f + \xi\frac{\partial f}{\partial \xi}, \quad \theta = 1, \quad \phi = 1, \tag{12}$$

$$\eta \to \infty : \mathrm{f}' \to 0, \quad \theta \to 0, \quad \phi \to 0, \tag{13}$$

where a prime denotes partial differentiation with respect to η and:

$$Ha^2 = \frac{\sigma B_o^2}{\rho v}\left(\frac{x_o^4}{Gr_{x_o}}\right)^{1/2}, \quad N = \frac{\beta_c(c_w - c_\infty)}{\beta_T(T_w - T_\infty)}, \quad \mathrm{Pr} = \frac{\nu}{\alpha}, \quad R_d = \frac{4\sigma T_\infty^3}{[k(a_r + \sigma_s)]}, \tag{14}$$

$$r_t = \frac{T_w}{T_\infty}, \quad Sc = \frac{\nu}{D}, \quad \gamma = k_r x_0^2/\upsilon(Gr_{x_0})^{1/2}, \quad f_o = \frac{v_o}{\nu}\left(\frac{x_o^4}{Gr_{x_o}}\right)^{1/4}$$

are the square of the Hartmann number, concentration to thermal buoyancy ratio, Prandtl number, radiation-conduction parameter, surface temperature parameter, Schmidt number, dimensionless chemical reaction parameter and mass transfer coefficient, respectively. In these definitions, $Gr_{x_o} = g\beta_T(T_w - T_\infty)\cos\Omega x_o^3/\nu^2$ is the Grashof number based on $\mathrm{x_o}$ and k is the thermal conductivity. It is should be noted that positive

values of f_0 indicate fluid suction at the cone surface while negative values of f_0 indicate fluid blowing or injection at the wall.

Equations (9)-(11) represent general equations which include various special cases. For example, by formally setting all of Ha, N and n equal to zero, equations (9) and (10) reduce to those reported earlier by Yih (1999) in his work concerning laminar natural convection over a truncated cone with uniform wall temperature and concentration the absence of a magnetic field and mass diffusion effect. Also, in the absence of chemical reaction ($\gamma = 0$), for constant wall temperature and concentration ($n = 0$), equations (9) and (10) reduce to those reported recently by Chamkha (2001).

The local skin-friction coefficient C_f, local Nusselt number $Nu_x{}^*$, and the local Sherwood number $Sh_x{}^*$ are important physical properties. These can be defined in dimensionless form below as given by Yih (1999) and Chamkha (2001):

$$C_f = -2(Gr_{x\bullet})^{-1/4} f''(\xi, 0), \quad Nu_{x\bullet} = -\left(1 + \frac{4R_d r_t^3}{3}\right)(Gr_{x\bullet})^{1/4}\theta'(\xi, 0)$$

$$Sh_{x\bullet} = -(Gr_{x\bullet})^{-1/4}\phi'(\xi, 0) \tag{15}$$

Numerical method

The initial-value problem represented by equations (9)-(13) with ξ playing the role of time is nonlinear and has no closed-form solution. Therefore, it must be solved numerically. The implicit, tri-diagonal, finite-difference method discussed by Blottner (1970) has proven to be adequate for the solution of boundary-layer equations accurately. For this reason, it is adopted in this work.

All first-order derivatives with respect to ξ are replaced by two-point backward difference quotients such that:

$$\frac{\partial A}{\partial \xi} = \frac{A_{m,n} - A_{m-1,n}}{\Delta\xi_{m-1}} \tag{16}$$

where A is a typical independent variable. m and n indicate lines of constant ξ and constant η, respectively. $\Delta\xi_{m-1}$ is the ξ step size between the $m - 1$ and m lines of constant ξ.

Equation (9) is converted into a second-order partial differential equation by letting $V = f'$. Then, all equations governing V, θ and ϕ can be written in the general form:

$$\pi_1 Z'' + \pi_2 Z' + \pi_3 Z + \pi_4 = 0 \tag{17}$$

where $Z = V$, θ, or ϕ and the π's are constants, functions of the dependent variables, or functions of the independent variables. These equations are discretized using three-point central-difference quotients and, as a consequence, a set of algebraic equations results at each line of constant ξ. These algebraic equations are then solved by the well-known Thomas algorithm (Blottner, 1970) with iteration to deal with the nonlinearities of the problem. When the solution at a specific line of constant ξ is obtained, the same solution procedure is used for the next line of constant ξ. This marching process continues until the desired value of ξ is reached. At each line of constant ξ, when V is known, the equation $f' = V$ is then solved for f using the trapezoidal rule. The convergence criterion employed was based on the difference between the current and the previous iterations.

When this difference reached 10^{-5}, the solution was assumed converged and the iteration procedure was terminated. Variable step sizes in the η-direction and constant step sizes in the ξ-direction were utilized in order to accommodate the sharp changes in the dependent variables especially in the immediate vicinity of the cone surface. The (ξ, η) computational domain consisted of 101 and 196 points, respectively. The constant step size in ξ was taken to be 10^{-2} while the initial step size in η was taken to be equal to 10^{-3} and the growth factor was taken to be 1.04. This gave $\eta_\infty = 150$. These values were found to give accurate grid-independent results as verified by the comparisons mentioned below.

In order to access the accuracy of the numerical results, various comparisons with the previously published work of Yih (1999) and Chamkha (2001) for the cases of a vertical plate ($\xi = 0$) and a full cone ($\xi = \infty$) were performed. These comparisons are presented in Tables I and II. It is obvious from these tables that excellent agreement between the results exist. These favourable comparisons lend confidence in the graphical results to be reported in the next section.

Results and discussion

In this section, a representative set of numerical results for the velocity, temperature, and concentration profiles as well as the local skin-friction coefficient, local Nusselt number and the local Sherwood number is shown graphically in Figures 2-19. These results illustrate the effects of the Hartmann number Ha, wall temperature and concentration exponent n, thermal radiation parameter R_d, dimensionless chemical reaction parameter

Table I.
Comparison of values of $f''(0, 0)$ and $-\theta'(0, 0)$ for various values of Pr with $f_o = 0$, $n = 0$, $Ha = 0$, $N = 0$, $\gamma = 0$ and $R_d = 0$

	$f''(0, 0)$			$-\theta'(0, 0)$		
Pr	Yih (1999)	Chamkha (2001)	Present results	Yih (1999)	Chamkha (2001)	Present results
0.0001	1.4998	1.4997	1.4997	0.0060	0.0059	0.0059
0.001	1.4728	1.4727	1.4727	0.0189	0.0188	0.0188
0.01	1.3968	1.3965	1.3965	0.0570	0.0574	0.0574
0.1	1.2144	1.2151	1.2151	0.1629	0.1630	0.1630
1	0.9084	0.9081	0.9081	0.4012	0.4015	0.4015
10	0.5927	0.5927	0.5927	0.8266	0.8274	0.8274
100	0.3559	0.3558	0.3558	1.5493	1.5503	1.5503
1,000	0.2049	0.2049	0.2049	2.8035	2.8044	2.8044
10,000	0.1161	0.1161	0.1161	5.0127	5.0131	5.0131

Table II.
Comparison of values of $f''(\infty, 0)$ and $-\theta'(\infty, 0)$ for various values of Pr with $f_o = 0$, $n = 0$, $Ha = 0$, $N = 0$, $\gamma = 0$ and $R_d = 0$

	$f''(\infty, 0)$			$-\theta'(\infty, 0)$		
Pr	Yih (1999)	Chamkha (2001)	Present results	Yih (1999)	Chamkha (2001)	Present results
0.0001	1.6006	1.6005	1.6005	0.0079	0.0078	0.0078
0.001	1.5135	1.5133	1.5133	0.0246	0.0245	0.0245
0.01	1.3551	1.3549	1.3549	0.0749	0.0751	0.0751
0.1	1.0960	1.0962	1.0962	0.2116	0.2116	0.2116
1	0.7699	0.7697	0.7697	0.5109	0.5111	0.5111
10	0.4877	0.4877	0.4877	1.0339	1.0342	1.0342
100	0.2896	0.2895	0.2895	1.9226	1.9230	1.9230
1,000	0.1661	0.1661	0.1661	3.4696	3.4700	3.4700
10,000	0.0940	0.0940	0.0940	6.1984	6.1988	6.1988

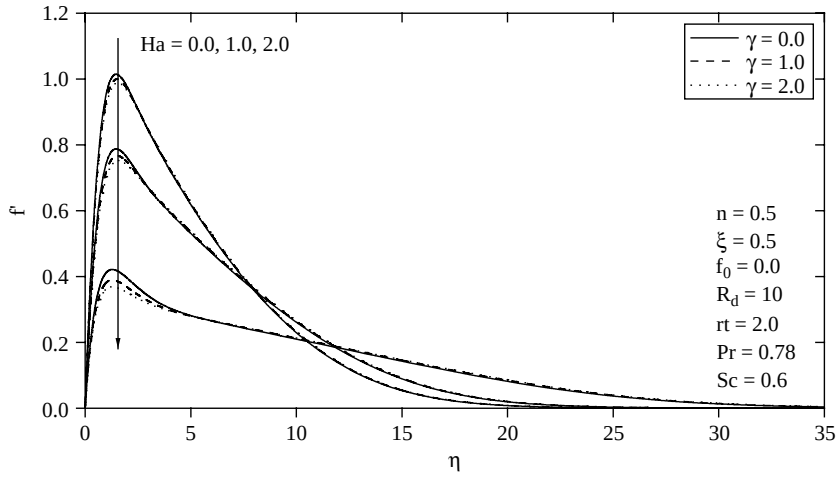

Figure 2.
Effects of Ha and γ on velocity profiles

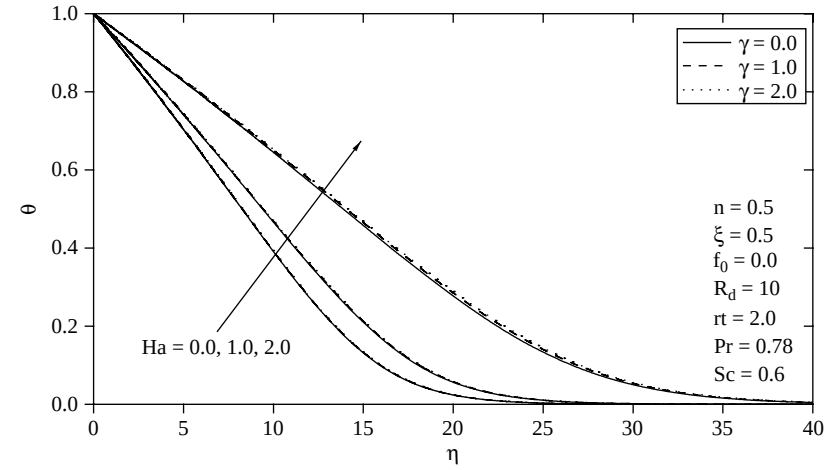

Figure 3.
Effects of Ha and γ on temperature profiles

γ, and the suction/injection parameter f_o on the solutions. Throughout the calculations, the conditions are intended for two electrically conducting fluids, metal ammonia suspensions (Pr = 0.78) and mercury (Pr = 0.027) polluted by water vapor (Sc = 0.6) that represents a diffusion chemical species of most common interest in water. The values of the corresponding buoyancy force parameter (ratio of the buoyancy force due to mass diffusion to the buoyancy force due to the thermal diffusion) N takes the value 1.0 for low concentration, at variable surface temperature and concentration the presence of a magnetic field and thermal radiation effects.

Figures 2-4 show typical profiles for the velocity along the cone f′, temperature θ and concentration ϕ for various values of the Hartmann number Ha and the chemical reaction parameter γ, respectively. Application of a magnetic field normal to the flow of an electrically conducting fluid gives rise to a resistive force called the Lorentz force which acts in the direction opposite to that of the flow. This resistive force tends to slow

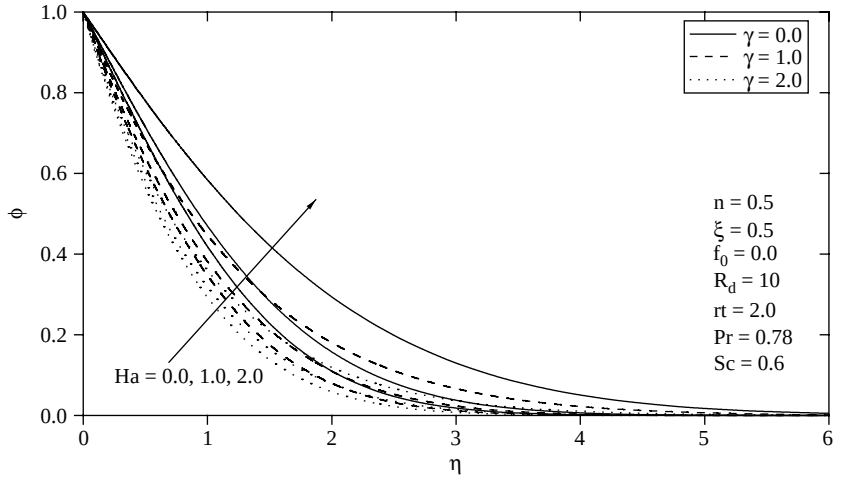

Figure 4.
Effects of Ha and γ on concentration profiles

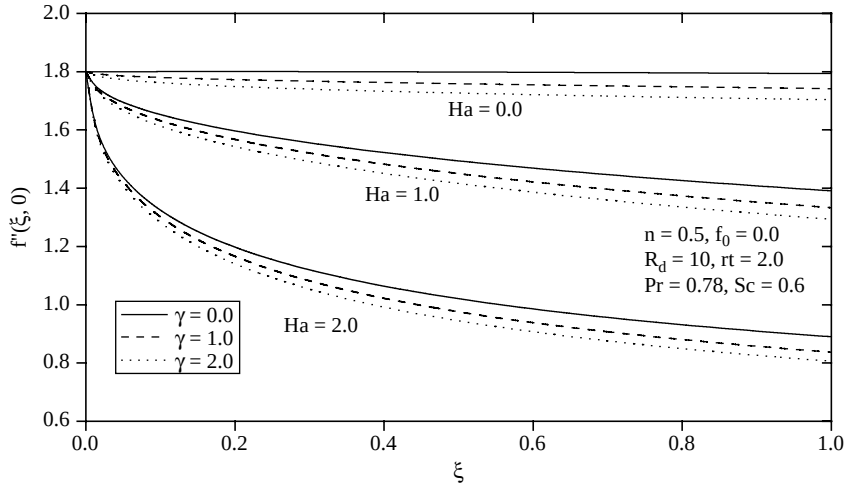

Figure 5.
Effects of Ha and γ on development of skin-friction coefficient

down the motion of the fluid along the cone and causes increases in its temperature and solute concentration. This is depicted by the decreases in the values of f′ and increases in the values of both θ, and ϕ as Ha increases shown in Figures 2-4. These behaviours in f′, θ, and ϕ are accompanied by increases in all of the hydrodynamic, thermal, and concentration boundary layers as Ha increases. On other hand, it is seen that the velocity and concentration profiles decrease with increases in the chemical reaction parameter, while a small change in the temperature profiles occurs. This shows that the diffusion rates can be tremendously altered by chemical reactions. It is also important to note that increasing the chemical reaction parameter significantly alters the concentration boundary layer thickness without any significant effect on the momentum and thermal boundary layers.

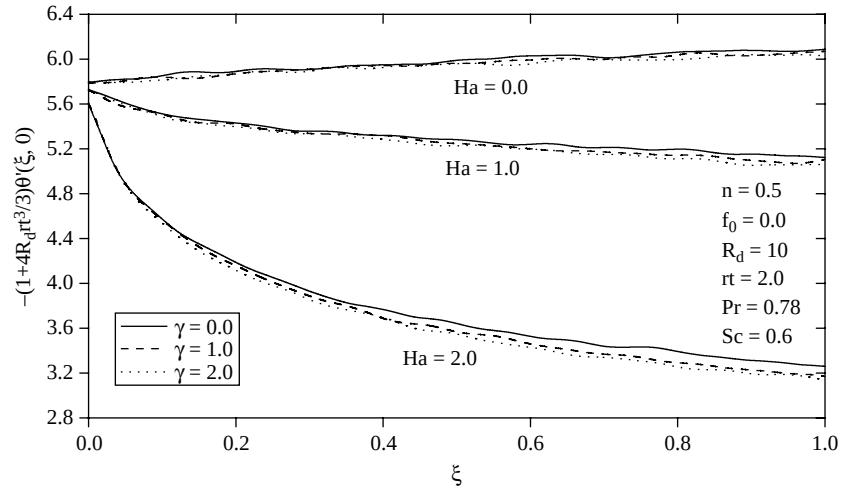

Figure 6.
Effects of Ha and γ on development of Nusselt number

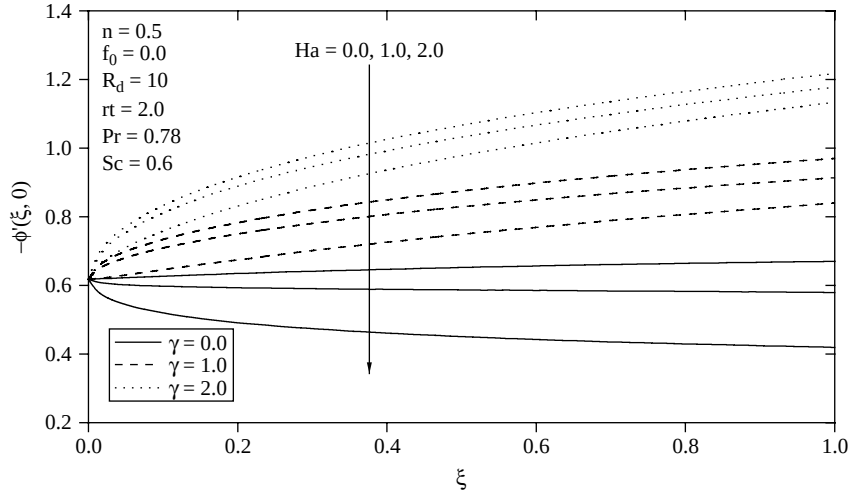

Figure 7.
Effects of Ha and γ on development of Sherwood number

Figures 5-7 show the effects of the Hartmann number Ha on the local skin-friction coefficient C_f, local Nusselt number $Nu_{x\bullet}$, and the local Sherwood number $Sh_{x\bullet}$, respectively. As seen from the definitions of C_f, $Nu_{x\bullet}$, and $Sh_{x\bullet}$, they are directly proportional to $f''(\xi, 0)$, $-\theta'(\xi, 0)$ and $-\phi'(\xi, 0)$, respectively. For this reason, they are shown in Figures 5-7. It was seen from Figures 2-4 that the wall slope of the velocity profile decreases while the slopes of both the temperature and concentration profiles increase as Ha increases. This produces reductions in all of C_f, $Nu_{x\bullet}$, and $Sh_{x\bullet}$ as Ha increases as shown in Figures 5-7. It is also observed from these figures that for $Ha = 2.0$ all of $f''(\xi, 0)$, $-\theta'(\xi, 0)$ and $-\phi'(\xi > , 0)$ decrease with increasing values of ξ while they increase with ξ for $Ha = 0$. Further, it can be seen that as γ increases, the local Sherwood

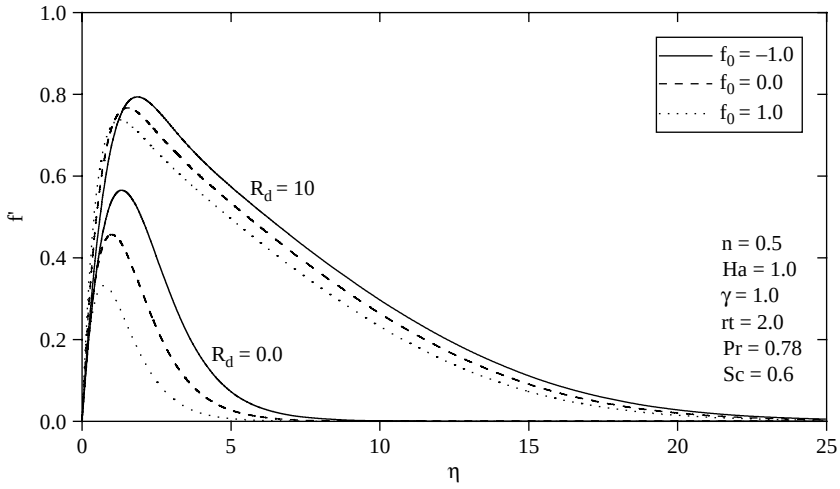

Figure 8.
Effects of f_o and R_d on velocity profiles

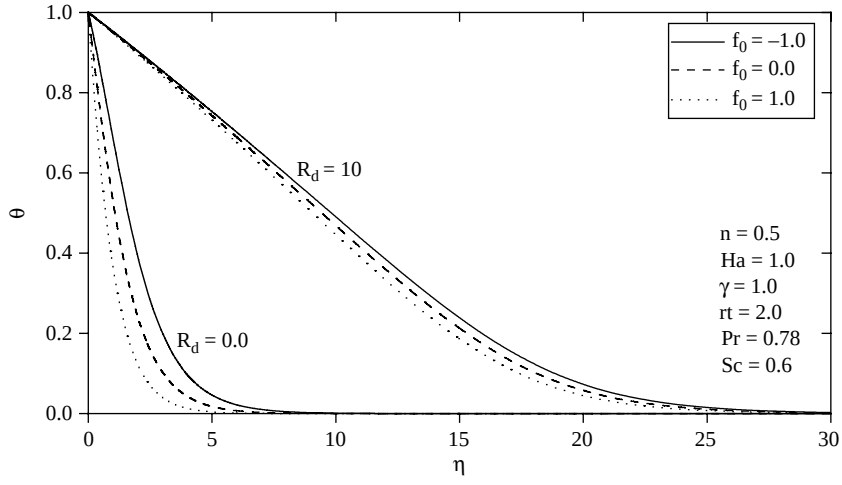

Figure 9.
Effects of f_o and R_d on temperature profiles

number increases while the opposite effect is found for both of the local skin-friction coefficient and the local Nusselt number. This is because as γ increases, the concentration difference between the cone surface and the fluid decreases and so the rate of mass transfer at the cone surface must increase while the skin-friction coefficient decrease as a result of the decrease in the flow velocity of the fluid.

Figures 8-10 show representative velocity, temperature and concentration profiles for various values of the wall mass transfer coefficient f_o and two values of the radiation-conduction parameter R_d, respectively. Imposition of fluid suction ($f_o > 0$) at the cone surface has a tendency to reduce all of the hydrodynamic, thermal and concentration boundary layers. This causes all of the velocity, temperature and concentration to decrease at every point far from the surface. On the other hand,

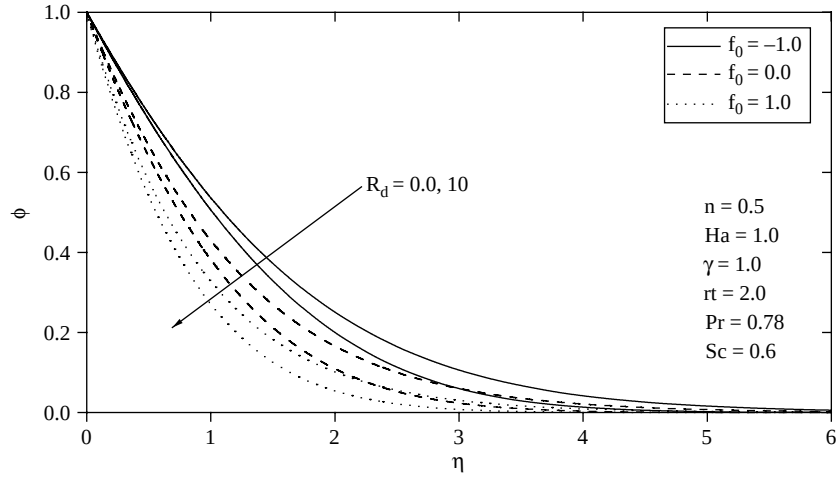

Figure 10.
Effects of f_o and R_d on concentration profiles

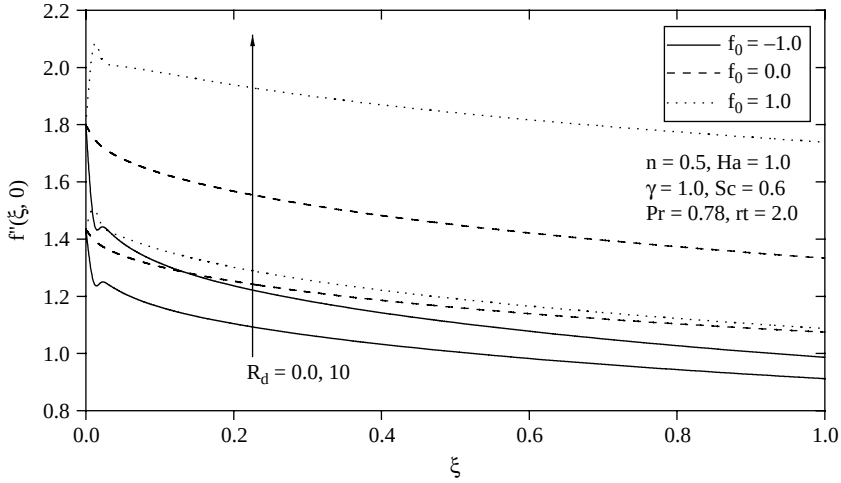

Figure 11.
Effects of f_o and R_d on development of skin-friction coefficient

injection of fluid ($f_o < 0$) through the cone surface produces the opposite effect, namely increases in all of the velocity, temperature and concentration. These behaviours are clearly shown in Figures 8-10. Consistent with the behaviour reported by Yih (1999) and Chamkha (2001), increasing the value of R_d results in increases in both the velocity and temperature distribution and the maximum velocity tends to move away from the cone surface. However, the concentration distribution tends to decrease as a result of increasing the radiation effect as observed from Figure 10.

The effects of both f_o and R_d on the development of the local skin-friction coefficient (or $f''(\xi, 0)$), the local Nusselt number (or $-\theta'(\xi, 0)$) and the local Sherwood number (or $-\phi'(\xi, 0)$) are shown in Figures 11-13, respectively. Inspection of the velocity, temperature and concentration profiles shown in Figures 8-10 reveals that $f''(0.5, 0)$

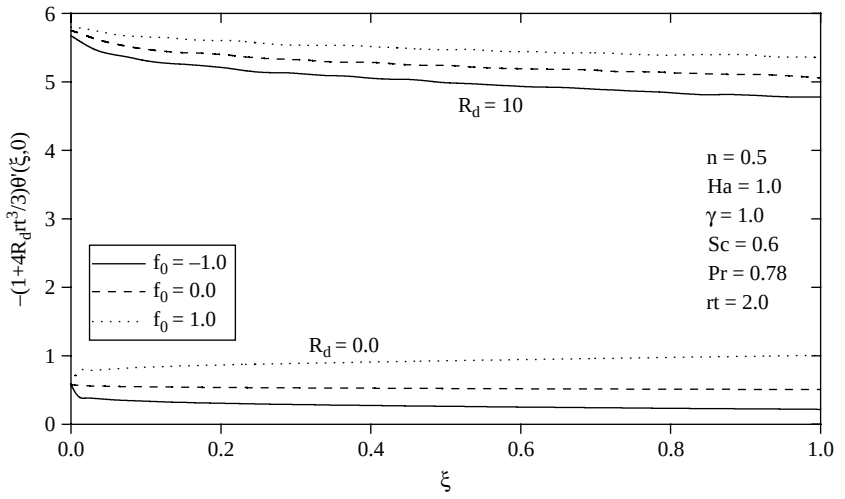

Figure 12.
Effects of f_o and R_d on development of Nusselt number

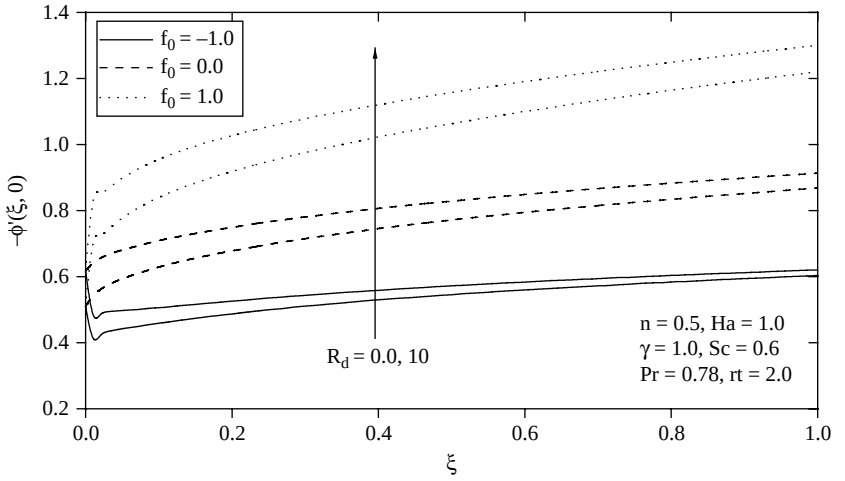

Figure 13.
Effects of f_o and R_d on development of Sherwood number

decreases for $R_d = 0$ and increases for $R_d = 10$ as f_o increases and $f''(0.5, 0)$ is higher for $R_d = 10$ than that of $R_d = 0$. The same behaviour apparently exists for other values of ξ with small overshoots and undershoots close to $\xi = 0$ and then a continuously decaying trend with ξ takes place. It also reveals that $-\phi'(0.5, 0)$ increases as either of f_o or R_d increases and that $-\phi'(\xi, 0)$ has a decaying trend with ξ for $f_o < 0$ and an increasing behaviour with ξ for $f_o > 0$ while it remains almost constant with ξ for $f_o = 0$. However, the behaviour of $-\theta'(\xi, 0)$ is somewhat different for $R_d = 0$ where it decreases and increases sharply with ξ for $f_o < 0$ and $f_o > 0$, respectively, while it remains almost constant for $f_o = 0$. The curve associated with $f_o = 1.0$ (for $R_d = 0$) lies outside the range of the figure and, therefore, is not shown. In addition, while for $R_d = 10$ the values of $-\theta'(\xi, 0)$ are lower than those corresponding to $R_d = 0$ for $f_o \geq 0$,

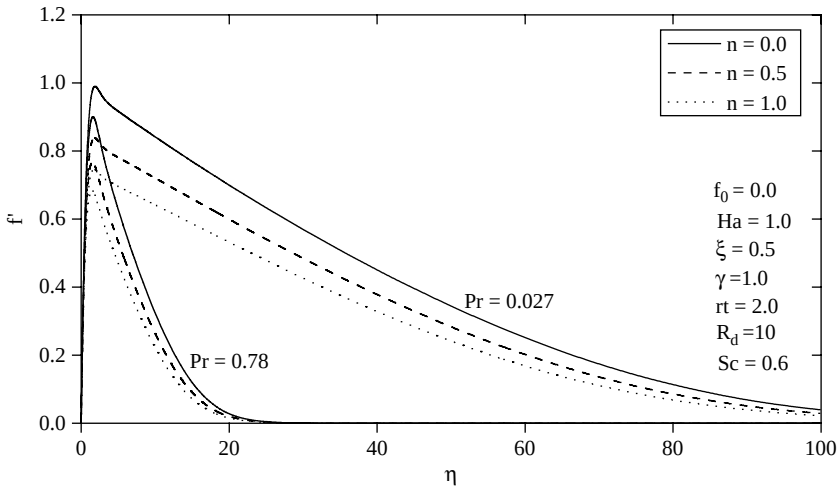

Figure 14.
Effects of Pr and n on velocity profiles

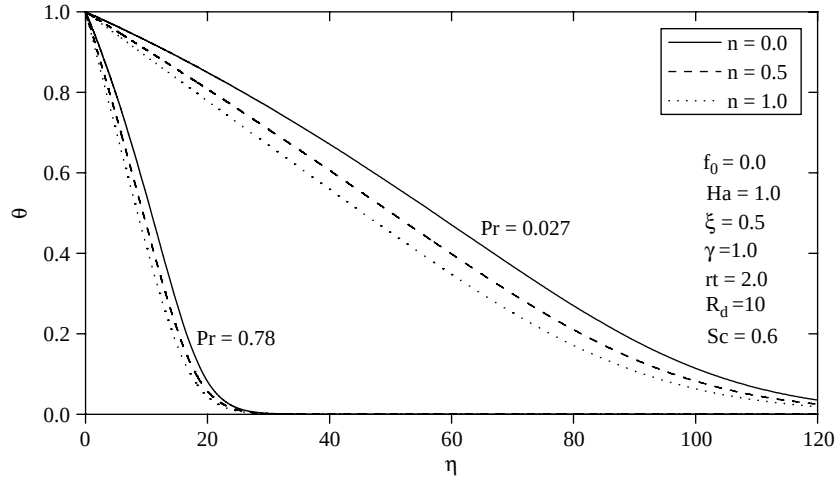

Figure 15.
Effects of Pr and n on temperature profiles

they are higher for $f_o < 0$ than those corresponding to $R_d = 0$ except at very small values of ξ. It should be mentioned that the behaviour of the local Nusselt number will be different than that shown in Figure 12 for $R_d = 10$ (as evident from equations (15)) where its values will be higher than those associated with $R_d = 0$ for all values of f_o. All of the above trends are evident from Figures 11-13.

Figures 14-16 show the effects of the wall temperature and concentration exponent n on the velocity, temperature, and concentration profiles at $\xi = 0.5$ for two values of the Prandtl number Pr corresponding to metal ammonia suspensions (Pr = 0.78) and mercury (Pr = 0.027), respectively. For a given value of Pr, an increase in the exponent n tends to decelerate the flow around the cone surface with reductions

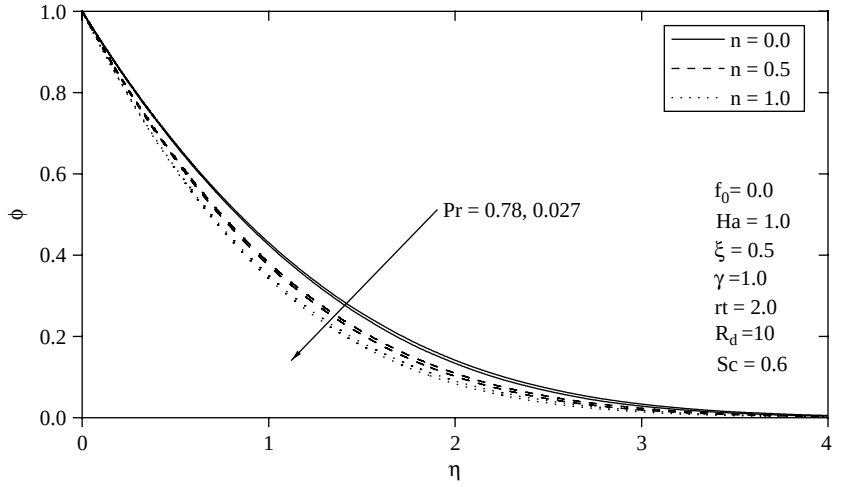

Figure 16.
Effects of Pr and n on concentration profiles

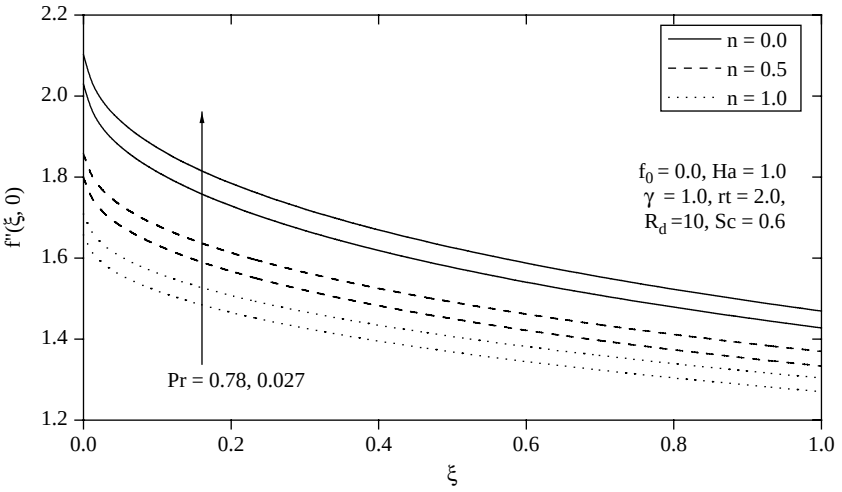

Figure 17.
Effects of Pr and n on development of skin-friction coefficient

in the temperature and concentration profiles as shown in Figures 14-16. Furthermore, it is observed from these figures that for a given value of n, both the velocity and temperature profiles as well as their boundary layers increase while slight decreases in the concentration profile and its boundary layer take place as Pr decreases.

In Figures 17-19, the effects of n and Pr on the values of C_f, $Nu_{x\bullet}$, and $Sh_{x\bullet}$ are presented, respectively. In these figures, it is predicted that, regardless of the value of Pr, an increase in the value of n results in a decrease in the local friction coefficient, in terms of C_f, while, higher heat transfer rates $Nu_{x\bullet}$ can be obtained by increasing the value of n for certain values of ξ. Moreover, it is seen that the mass transfer is enhanced by increasing the value of n. This can be explained from Figure 14, where it is clearly seen that for Pr = 0.027, the wall slopes of the velocity profiles become steep and

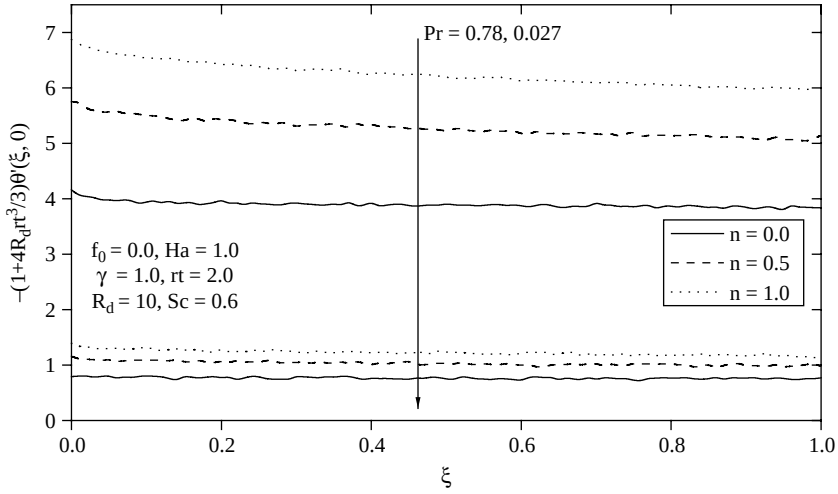

Figure 18.
Effects of Pr and n on development of Nusselt number

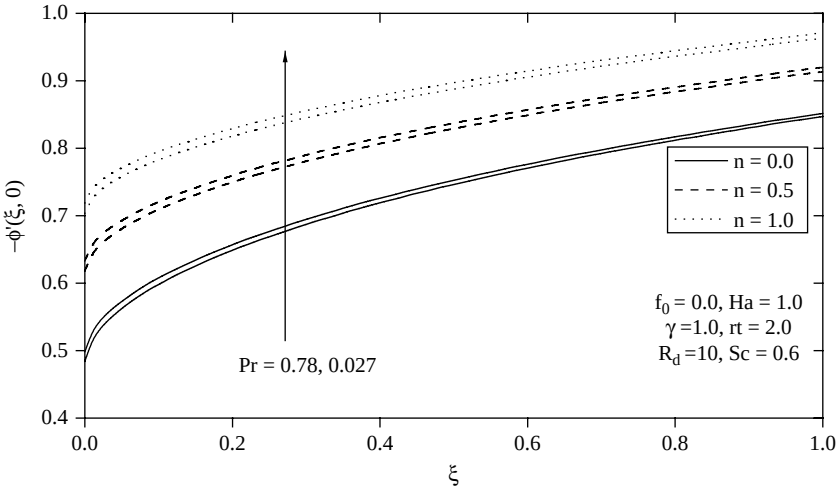

Figure 19.
Effects of Pr and n on development of Sherwood number

slightly increased as n increases while they are clearly reduced for $Pr = 0.78$. The effect of reducing the value of Pr is observed to increase the values of both C_f and $Sh_{x\bullet}$ and to decrease the values of $Nu_{x\bullet}$. It should also be noted that the increase in the local Nusselt number due to increasing the exponent n is more pronounced for a larger Prandtl number such as that corresponding to metal ammonia suspensions while it is lower for moderate values of the Prandtl number such as that for mercury. This can be explained from the fact that as the Prandtl number increases, the thermal boundary-layer thickness decreases and the wall temperature gradient increases. This is true for all values of ξ as evident from Figures 17-19.

Conclusion

The problem of steady-state, laminar heat and mass transfer by natural convection boundary-layer flow around a permeable truncated cone with variable surface temperature and concentration in the presence of magnetic field, thermal radiation and chemical reaction effects was considered. A set of non-similar governing differential equations was obtained and solved numerically by an implicit finite-difference methodology. Comparisons with previously published work on various special cases of the general problem were performed and the results were found to be in excellent agreement. A representative set of numerical results for the velocity, temperature and concentration profiles as well as the local skin-friction coefficient, local Nusselt number and the local Sherwood number was presented graphically and discussed. It was found that, in general, all of the local skin-friction coefficient, local Nusselt number and the local Sherwood number reduced as the magnetic Hartmann number was increased. Also, while all of these physical parameters decreased with the distance along the cone surface in the presence of the magnetic field, they increased with it in the absence of the magnetic field. It was also found that owing the increasing of wall temperature and concentration exponent, both of the local Nusselt number and the local Sherwood number increased while the opposite trend is observed for the local skin-friction coefficient. In addition, for a given value of the power-law exponent, it was observed that the increase in the local Nusselt number due to the exponent n was more pronounced for a larger Prandtl number such as that corresponding to metal ammonia suspensions while it was lower for moderate values of the Prandtl number such as that for mercury. Furthermore, both of the local skin-friction coefficient and Sherwood number were reduced while the local Nusselt number was enhanced as the Prandtl number increased. The effects of fluid suction at the cone surface was found to decrease the local skin-friction coefficient in the absence of thermal radiation effects and to increase it when the radiation effects were present. However, both the local Nusselt and Sherwood numbers were found to increase as the suction velocity was increased irregardless of the presence or absence of thermal radiation effects. Finally, the presence of the chemical reaction effect caused both of the local skin-friction coefficient and the local Nusselt number to decrease while the local Sherwood number increased.

References

Afify, A.A. (2004), "The effect of radiation on free convective flow and mass transfer past a vertical isothermal cone surface with chemical reaction in the presence of a transverse magnetic field", *Can. J. Phys.*, Vol. 82, pp. 447-58.

Andersson, K.I., Hansen, O.R. and Holmedal, B. (1994), "Diffusion of a chemically reactive species from a stretching sheet", *Int. J. Heat Mass Transfer*, Vol. 37, pp. 659-64.

Anjalidevi, S.P. and Kandasamy, R. (1999), "Effect of chemical reaction, heat and mass transfer on laminar flow along a semi infinite horizontal plate", *Heat Mass Transfer*, Vol. 35, pp. 465-7.

Anjalidevi, S.P. and Kandasamy, R. (2000), "Effects of chemical reaction heat and mass transfer on MHD flow past a semi infinite plate", *Z. Angew. Math. Mech.*, Vol. 80, pp. 697-701.

Blottner, F.G. (1970), "Finite-difference methods of solution of the boundary-layer equations", *AIAA J.*, Vol. 8, pp. 193-205.

Chamkha, A.J. (2001), "Coupled heat and mass transfer by natural convection about a truncated cone in the presence of magnetic field and radiation effects", *Numer. Heat Transfer, Part A*, Vol. 39, pp. 511-30.

Chamkha, A.J. (2003), "MHD flow of a uniformly stretched vertical permeable surface in the presence of heat generation/absorption and a chemical reaction", *Int. Commun. Heat Mass Transfer*, Vol. 30, pp. 413-22.

Chamkha, A.J. and Al-Mudhaf, A. (2004), "Simultaneous heat and mass transfer from a permeable sphere at uniform heat and mass fluxes with magnetic field and radiation effects", *Numer. Heat Transfer, Part A*, Vol. 46, pp. 181-98.

Cheng, C.Y. (2008), "Natural convection of a micropolar fluid from a vertical truncated cone with power-law variation in surface temperature", *Int. Commun. Heat Mass Transfer*, Vol. 35, pp. 39-46.

Cheng, C.Y. (2009), "Natural convection heat and mass transfer from a vertical truncated cone in a porous medium saturated with a non-Newtonian fluid with variable wall temperature and concentration", *Int. Commun. Heat Mass Transfer*, Vol. 36, pp. 585-9.

Das, U.N., Deka, R.K. and Soundalgekar, V.M. (1994), "Effects of mass transfer on flow past an impulsively started infinite vertical plate with constant heat flux and chemical reaction", *Forsch. Ingenieurwes. Eng. Res.*, Vol. 60, pp. 284-7.

Gebhart, B., Jaluria, Y., Mahajan, R.L. and Sammakia, B. (1998), *Buoyancys-induced Flow and Transport*, Hemisphere, New York, NY.

Ibrahim, F.S., Elaiw, A.M. and Bakr, A.A. (2008), "Effect of the chemical reaction and radiation absorption on the unsteady MHD free convection flow past a semi infinite vertical permeable moving plate with heat source and suction", *Commun. Nonlinear Sci. Numer. Simulat.*, Vol. 13, p. 1056.

Kandasamy, R., Periasamy, K. and Sivagnana Prabhu, K.K. (2005), "Chemical reaction, heat and mass transfer on MHD flow over a vertical stretching surface with heat source and thermal stratification effects", *Int. J. Heat Mass Transfer*, Vol. 48, pp. 4557-61.

Mohamed, R.A. and Abo-Dahab, S.M. (2009), "Influence of chemical reaction and thermal radiation on the heat and mass transfer in MHD micropolar flow over a vertical moving porous plate in a porous medium with heat generation", *Int. J. Thermal Sci.*, Vol. 48, pp. 1800-13.

Muthucumaraswamy, R. and Ganesan, P. (1998), "Unsteady flow past an impulsively started vertical plate with heat and mass transfer", *Heat Mass Transfer*, Vol. 34, pp. 187-93.

Muthucumarswamy, R. and Ganesan, P. (2001), "First order chemical reaction on flow past an impulsively started vertical plate with uniform heat and mass flux", *Acta Mech.*, Vol. 147, p. 45.

Muthucumarswamy, R. and Ganesan, P. (2002), "Effects of suction on heat and mass transfer along a moving vertical surface in the presence of chemical reaction", *Forsch. Ingenieurwes.*, Vol. 67, p. 129.

Na, T.Y. and Chiou, J.P. (1979), "Laminar natural convection over a frustum of a cone", *Appl. Sci. Res.*, Vol. 35, pp. 409-21.

Pal, D. and Talukdar, B. (2010a), "Buoyancy and chemical reaction effects on MHD mixed convection heat and mass transfer in a porous medium with thermal radiation and Ohmic heating", *Commun. Nonlinear Sci. Numer. Simulat.*, Vol. 15, pp. 2878-93.

Pal, D. and Talukdar, B. (2010b), "Perturbation analysis of unsteady magnetohydrodynamic convective heat and mass transfer in a boundary layer slip flow past a vertical permeable plate with thermal radiation and chemical reaction", *Commun. Nonlinear Sci. Numer. Simulat.*, Vol. 15, pp. 1813-30.

Pop, I. and Na, T.Y. (1999), "Natural convection over a vertical wavy frustum of a cone", *Int. J. Non-Linear Mech.*, Vol. 34, pp. 925-34.

Postelnicu, A. (2006), "Free convection about a vertical frustum of a cone in a micropolar fluid", *Int. J. Eng. Sci.*, Vol. 44, pp. 672-82.

Rashad, A.M. (2008), "Influence of radiation on MHD free convection from a vertical flat plate embedded in porous media with thermophoretic deposition of particles", *Commun. Nonlinear Sci. Numer. Simulat.*, Vol. 13, pp. 2213-22.

Seddeek, M.A. (2005), "Finite-element method for the effects of chemical reaction, variable viscosity, thermophoresis and heat generation/absorption on a boundary-layer hydromagnetic flow with heat and mass transfer over a heat surface", *Acta Mech.*, Vol. 177, pp. 1-18.

Soundalgekar, V.M. (1977), "Free convection effects on the stokes problem for infinite vertical plate", *ASME J. Heat Transfer*, Vol. 99, pp. 499-501.

Yih, K.A. (1999), "Effect of radiation on natural convection about a truncated cone", *Int. J. Heat Mass Transfer*, Vol. 42, pp. 4299-305.

Corresponding author
Ali J. Chamkha can be contacted at: achamkha@yahoo.com